Dynamic SPECT Evaluation of Renal Plasma Flow Using Technetium-99m MAG3 in Kidney Transplant Patients

Hideaki Akahira, Harue Shirakawa, Hanjiro Shimoyama, Megumi Tsushima, Hideo Arima, Kazuo Nigawara, Tomihisa Funyu, Motoaki Sato and Tadashi Suzuki

Translation from Japanese by Iku Burns

Department of Radiology, Oyokyo Kidney Research Institute, Hirosaki; and Department of Urology, Hirosaki University School of Medicine, Hirosaki, Japan

Objective: The purpose of this study was to evaluate Patlak's graphic analysis method to determine renal plasma flow (RPF) in kidney transplants.

Methods: Dynamic SPECT was performed with ^{99m}Tc MAG3 in 12 patients. RPF was determined by both Patlak's graphic analysis method and Russell's method. Ventral, central and dorsal tomographic images of the transplanted kidney were reconstructed to estimate intrarenal distribution of renal plasma flow.

Results: The renal influx constant (Ku) calculated by Patlak's graphic analysis method was reproducible and correlated with both serum creatinine ($r = -0.88$, $P < 0.001$) and blood urea nitorogen levels ($r = -0.82$, $P < 0.002$). However, a significant difference was noted between the RPF values derived from Patlak's graphic analysis method and Russell's method. Ku was corrected by a factor calculated from raw and reconstructed data, and the resulting values were in fair agreement with those determined by Russell's method.

Conclusion: These methods are useful in evaluating the function of transplanted kidneys.

Key Words: renal plasma flow methods; dynamic SPECT; renal transplant

J Nucl Med Technol 1999; 27:32–37

Technetium-99m MAG3 (mercaptoacetyltriglycine, mertiatide) was developed for performing dynamic renal scintigraphy. It is secreted mainly by the renal tubular cells, similar to orthoiodohippurate(OIH) (*1*). Many studies have been published using ^{99m}Tc MAG3 for determining effective renal plasma flow (ERPF). These include the renal count method with planar images by Schlegel et al. (*2*) and Ito et al. (*3*), and the blood clearance method by Tauxe et al. (*4*) and Russell et al. (*5*). Gjedde et al. (*6*) and Patlak et al. (*7*) reported the graphic analysis method, which has been used for determining blood flow in various organs. The Patlak (*7*) method has been used most widely. If there is no tracer redistribution between blood and tissue, blood flow of any organ, except brain, could be calculated from the total volume and the arterial tracer concentration in that organ.

The Patlak method (*7*) was applied to our ^{99m}Tc MAG3 dynamic SPECT (D-SPECT), and was evaluated as a method to estimate the intrarenal distribution of renal plasma flow (RPF) on three tomographic views of transplanted kidneys along with the calculation of total ERPF. The reliability of this method was investigated, as well as the correlation among ERPF, serum creatinine (SCr) and blood urea nitrogen (BUN) by the clearance method (*5*) in renal transplant patients. Reproducibility also was evaluated.

According to Patlak's theoretical model of blood-tissue tracer exchange (*7*), the unidirectional, intrarenal tracer concentration, B(t), in the initial circulation from blood to kidney is as follows (*8*):

$$B(t) = Ku \int_0^t A(t)dt + Vn \times A(t), \qquad \text{Eq. 1}$$

where:

Ku is a renal influx rate constant;
A(t) is the arterial tracer concentration at the time t; and
Vn is an initial nonspecific distribution volume in the kidney.

Equation 1 divided by A(t) yields:

$$B(t)/A(t) = Ku \int_0^t A(t)dt/A(t) + Vn. \qquad \text{Eq. 2}$$

A Patlak plot is created by plotting B(t)/A(t) on the y-axis and $\int_0^t A(t)dt/A(t)$ on the x-axis. Ku is the slope of a straight line and Vn is the y-intercept of the line (Fig. 1).

For correspondence or reprints contact: Keisuke Kanao, *Japanese Journal of Nuclear Medicine Technology*, A507, 2–1-7, Satsukigaoka, Ikeda-shi, 563–0020 Osaka, Japan.

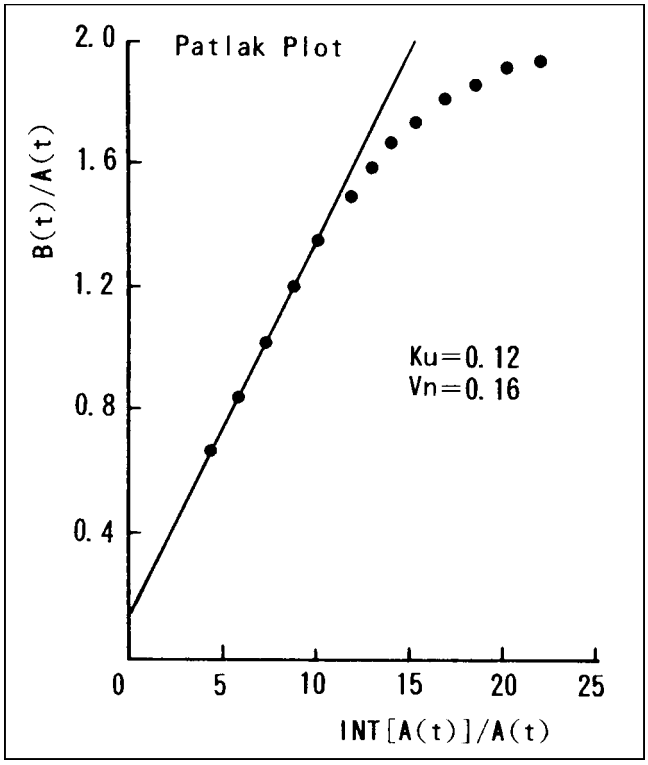

FIGURE 1. Example of a Patlak Plot. Ku is the slope of the straight line and Vn is the y-intercept of the line.

When the time-activity curve (TAC) of the cardiac region is substituted for A(t), the cardiac output (CO) per minute is assumed as total blood volume (TBV), then:

$$\text{Renal blood flow} = \text{TBV} \times \text{Ku} = \text{CO} \times \text{Ku}, \quad \text{Eq. 3}$$

when Equation 3 is corrected by the patient's hematocrit (Hct):

$$\text{Renal plasma flow} = \text{RBF} \times (1 - \text{Hct}). \quad \text{Eq. 4}$$

Total blood volume is calculated based on the weight and height of a patient (*9*).

MATERIALS AND METHODS

Eleven men and 1 woman who were 7–102 mo post renal transplant with various degrees of renal function had D-SPECT imaging. The age range was 21–42 y. The donors were either the mother (11 patients) or the father (1 patient).

Thirty minutes after hydration with 300 mL of water, 555 MBq ^{99m}Tc MAG3 were administered as an intravenous bolus. Dynamic SPECT imaging was performed immediately using a low-energy high-resolution collimator for 15 min with the heart and the transplanted kidney in the field of view. A 64 × 64 matrix was used and data were acquired over a 360° rotation for 30 s per frame.

After preprocessing the data with a 9-point smoothing routine, a ramp filter was applied and 30 sequential ventral tomographic images were constructed (30 s/frame). Time-smoothing was performed then. Chang attenuation correction ($\mu = 0.1$) was used (*10*).

The time-activity curve obtained from the average counts per voxel in the heart region of interest (ROI) was substituted for A(t) in Equation 2. The approximate value of this curve was calculated in relation to the biexponential function. B(t) was obtained by setting up the time-activity curve from the average counts per voxel in the ROI in the kidney. The background was defined over the superior pole of the kidney, and then 7-point time smoothing was performed.

There were differences between raw counts in the heart ROI (H-1) and in the reconstruction ROI of heart (H-1 recon) and between the raw kidney (K-1) data and reconstruction kidney (K-1 recon) data which were obtained from sequential ventral tomographic images (Fig. 2). These also varied from patient to patient. K-1, K-1 recon, H-1 and H- 1 recon were recalculated by adding all 15-min values for each time-activity curve. They were labeled as K raw, K recon, H raw and H recon, respectively, and a factor α was calculated:

$$\alpha = \frac{\text{K recon}}{\text{H recon}} \times \frac{\text{H raw}}{\text{K raw}}. \quad \text{Eq. 5}$$

Total RPF was obtained from corrected A(t) which was A(t) multiplied by factor α. The regional RPF values from three sections (ventral, central and dorsal) were processed by a previously reported method (*11*). The total RPF and the three sectional Ku value ratios were calculated.

Russell's blood clearance RPF method was performed (*5*).

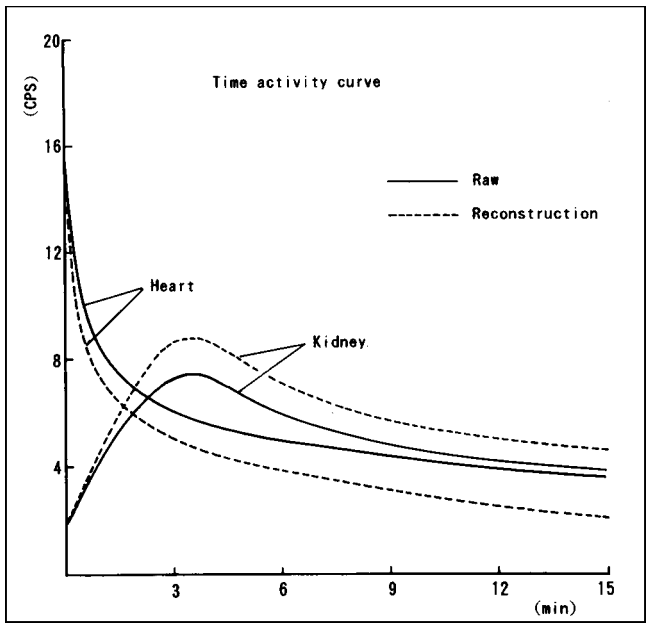

FIGURE 2. Time-activity curves from the ROIs over the heart and transplanted kidney. Raw count time-activity curves and reconstruction count time-activity curves are shown.

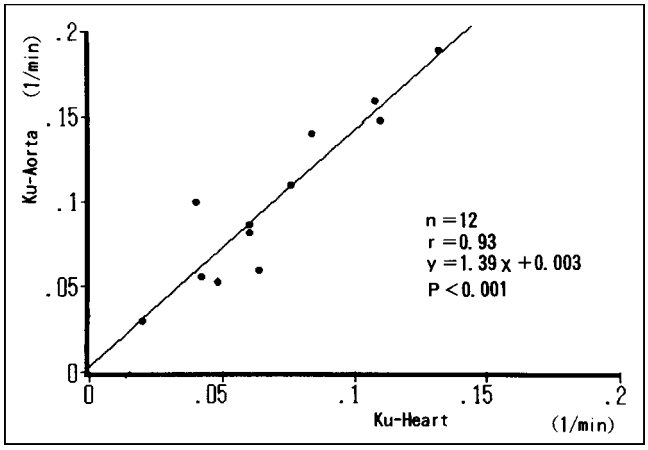

FIGURE 3. Comparison between the blood radioactivity value of arterial input location and Ku.

The activity of each control (10,000-fold dilution of the same amount of ^{99m}Tc MAG3 injected) and the centrifuged serum (3 mL blood drawn from the contralateral antecubital vein at 44 min. post ^{99m}Tc MAG3 injection) were measured in a well counter. Technetium-99m MAG3 clearance (MAG3 C) was calculated:

$$\text{MAG3 C} = \text{F max}\,(1 - e^{-a(1/c\,-\,\text{V lag})}), \qquad \text{Eq. 6}$$

and in the case of blood drawn at 44 min. postinjection:

$$\text{F max} = 632 \text{ (mL/min.)}$$

$$a = 0.0138\ (\Lambda^{-1})$$

$$\text{V lag} = 6.33 \text{ (L)}$$

C = cpm per 1 L serum/cpm per 1 mL control then:

$$\text{Renal plasma flow} = 632\,(1 - e^{-0.0138\,(1/C-6.33)}). \qquad \text{Eq. 7}$$

The Student t test was used for statistical evaluation. When P was less than 0.05, the result was considered significant.

RESULTS

Figure 3 shows the correlation ($r = 0.93$, $P < 0.001$) between Ku values when the input function of total blood volume was substituted by data from the heart and from the abdominal aorta. Figure 4 shows the correlation between the Ku method uncorrected A(t) and the Russell method ($r = 0.90$, $P < 0.001$). However, as the regression equation indicates ($y = 2.66x - 194$), there was a significant difference between the values obtained by the two methods. By using a corrected function A(t), the equation became $y = 0.97x - 7.43$ ($r = 0.93$, $P < 0.001$). The results were closer and had better correlation.

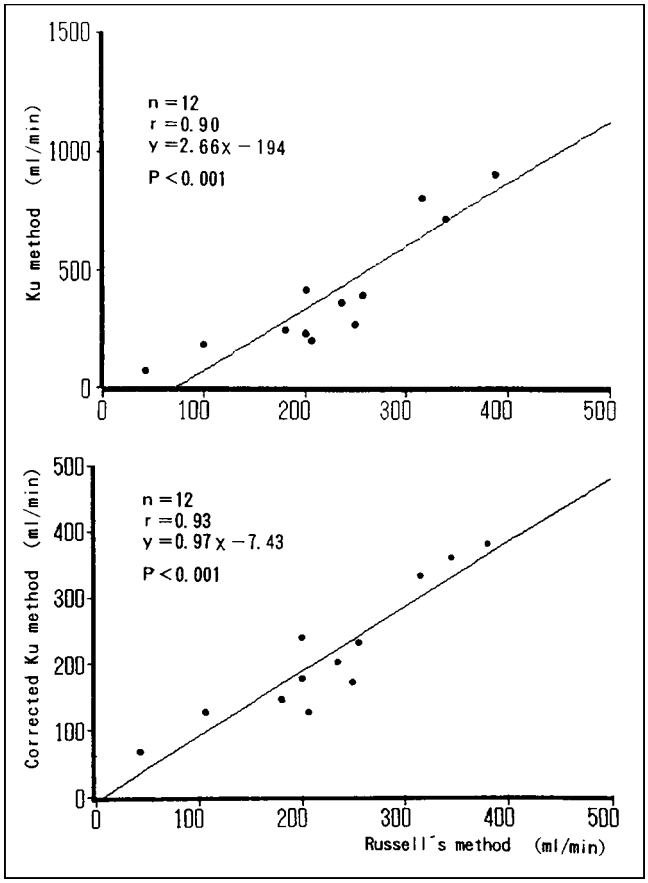

FIGURE 4. Comparison of renal plasma flow as determined by the Ku method, with and without correction, and the Russell method.

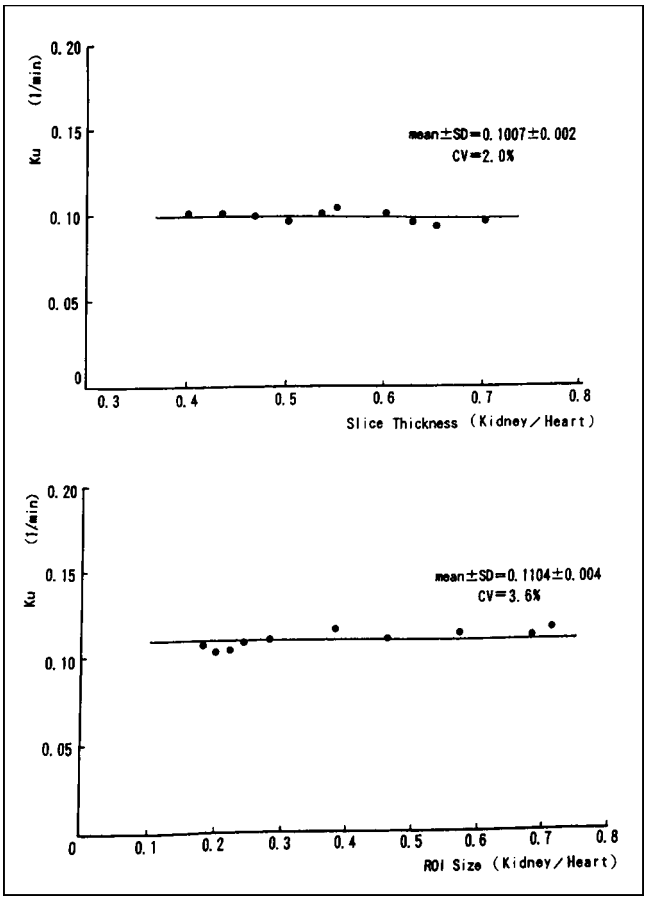

FIGURE 5. Effect of the ratio of slice thickness and area of ROI on Ku value.

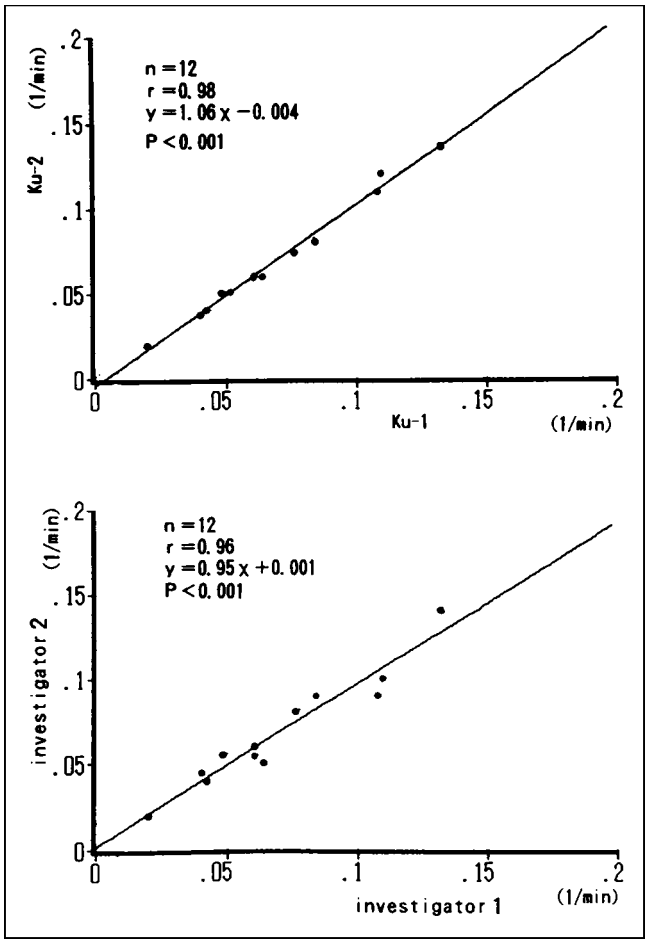

FIGURE 6. Intra- and interoperator reproducibility of the Ku value.

Figure 5 shows the effect of slice thickness on Ku value for the same data processing. The variation coefficient was 2.0%. The variation coefficient for ROI area was 3.6%.

Figure 6 gives the intra- and interinvestigator accuracy for determining the Ku value. They were r = 0.98 and r = 0.96, respectively. When the fluctuation coefficient at Ku value = 0.1 was calculated from the standard deviation of the circumference on the regression line, it was 3.7% for intrainvestigator and 8.6% for the interinvestigators.

Figure 7 shows the negative correlation found between Ku values and log SCr measured at the same time ($r = -0.88$, $P < 0.001$), and between Ku values and log BUN ($r = -0.82$, $P < 0.002$). There also was negative correlation between Ku values on three renal tomograms and log SCr($r = -0.78$ to -0.85, $P < 0.01$ to 0.001).

Figure 8 shows a representative example of a patient with a good prognosis. His SCr was 1.3 mg/dL (normal range = 0.7–1.7), BUN was 20 mg/dL (normal range = 8–22), and his creatinine clearance was 71 mL/min (normal range = 60–80). The RBF was 604 mL/min (normal range = 400–650) and the RPF was 338 mL/min (normal range = 200–400). Renal ventral, central and dorsal tomographic images of the transplanted kidney reconstructed after D-SPECT are shown. The RPFs for the three tomograms were 113, 175 and 100 mL/min., respectively. The central section had a higher RPF compared with the ventral and the dorsal sections.

Figure 9 shows a patient diagnosed with a renal infarct. His SCr remained elevated at 1.9 mg/dL. Technetium-99m DATA planar imaging (Fig. 9A) showed the defect in the central section of the kidney. Intravenous digital subtraction angiography (Fig. 9B) showed the infarct in the central artery of the three branches which enter the kidney and decreased blood flow in the distribution area of the artery. The tomographic three-sectional renal images by D-SPECT (Fig. 9C) also demonstrated the decreased accumulation of radiotracer and defects in the upper ventral, lateral central and central dorsal sections. The total RPF was 124 mL/min, and RPF was 197 mL/min. The RPF of each section was decreased as the ventral = 37 mL/min, the central = 45 mL/min and the dorsal = 42 mL/min.

DISCUSSION

We previously reported that D-SPECT data obtained with ^{99m}Tc DTPA applied to Rutland's glomerular filtration rate (GFR) method was useful in evaluating segmental renal transplant function (*11*). Although we assumed that we also could evaluate the renal blood flow (RBF) with this method, we could not.

Using D-SPECT data obtained with ^{99m}Tc MAG3 applied to

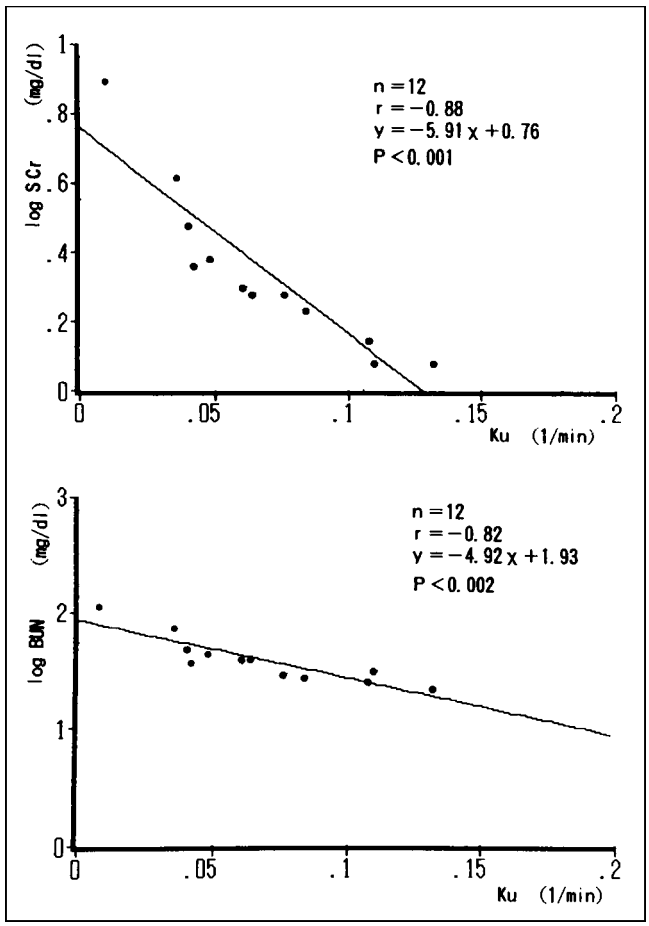

FIGURE 7. Correlation between Ku value, SCr and BUN.

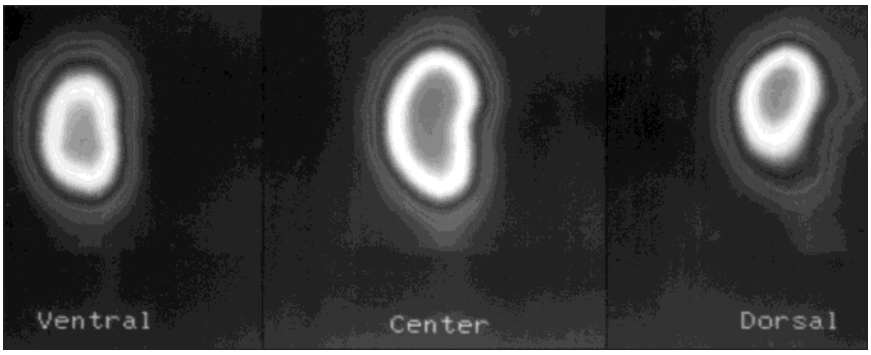

FIGURE 8. D-SPECT ventral, center and dorsal tomographic images of a well-functioning transplated kidney. The patient was a 42-y-old man who was 8 y postrenal transplant.

Patlak's graphic analysis, we attempted to calculate the total and segmental RPF from the renal influx rate constant (Ku). The Ku values obtained by this method had good reproducibility, correlated well with SCr and BUN, and we confirmed the usefulness of this application for the evaluation of renal transplant function. The reasons for the good reproducibility were:

Linear approximation of time zone (1.2–2.5 min.) matched with the functional phase of a renogram;
Input curve became stable with integral calculation;
Average counts per voxel became stable with 30 s acquisition per frame; and
The influence of ROI and slice thickness was low.

When we compared the RPF calculated by the Ku method with the Russell method, the correlation was good although the values by the Ku method were generally higher. For this reason, in the comparison of raw and reconstructed data, we speculated that the reconstruction data underestimated the heart because of rapid tracer washout, and overestimated the kidney because of variation in tracer accumulation during the functional phases (Fig. 2). Since the counts in the reconstruction data were proportional to the total counts in raw data, the correction coefficient α was obtained from each set of ROI projection data (α varied between 1.11 and 2.56). In addition, the integration value of each reconstructed time-activity curve was obtained and multiplied by A(t). Although the validity of this correction method should be evaluated further, the correlation between the two methods improved.

We also applied the previously reported method of using tomograms to estimate the local RPF in the kidney from the

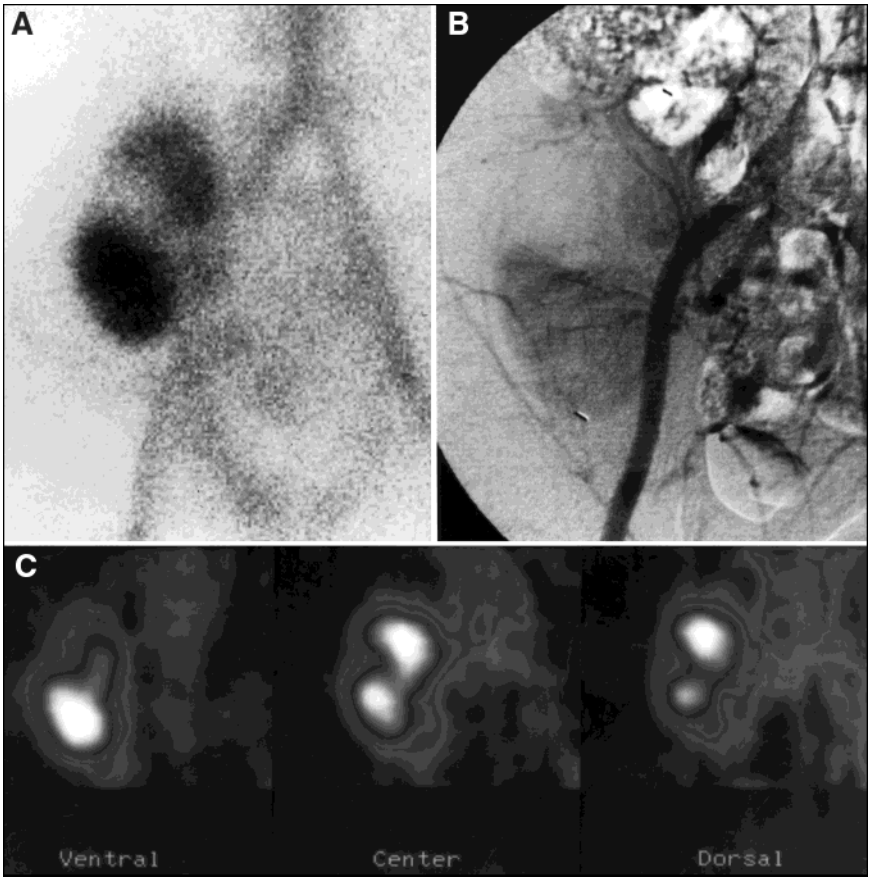

FIGURE 9. The patient was a 37-y-old man who had an infarct of his renal transplant. (A) Technetium-99m DTPA image demonstrating the renal infarct. (B) Intravenous digital subtraction angiography demonstrating the arterial infarct. (C) D-SPECT ventral, center and dorsal tomographic images demonstrating the renal infarct.

total RPF (*11*). We found that the central section always had the greatest counts in patients with a well-functioning kidney transplant. This also was seen with GFR determinations previously (*7*). This is due to the large volume of blood vessels in the central section of the kidney. Obtaining a stabilized renal long-axis image is difficult, however, when frontal tomographic images are being processed. A good understanding of the blood vessel distribution in each renal transplant is essential until a better method is developed. We also were able to numerically express decreased blood flow, as in the example case with a renal infarction.

CONCLUSION

We measured the total and regional RPF in renal transplant patients using Patlak's graphic analysis on D-SPECT data obtained with ^{99m}Tc MAG3. The Ku value had good reproducibility and was well correlated with SCr and BUN, although there was a significant difference between RPF calculated by the Ku method compared with Russell's method. The correction of the cardiac and renal ROI raw data in each case with the addition of the reconstructed time-activity curve minimized the difference. Regional RPF was obtained from tomograms that were divided into the three sections (ventral, central and dorsal). The central section had a higher RPF compared with the ventral or dorsal sections in well-functioning kidneys. The location and the degree of decreased blood flow in a kidney was numerically detected, which makes this method useful.

ACKNOWLEDGMENTS

This paper was originally published in the *Japanese Journal of Nuclear Medicine Technology* in Japanese. Keisuke Kanao selected this paper for translation and Iku Burns, CNMT, provided the translation.

REFERENCES

1. Fritzberg AR, Kasina S, Eshima D, Johnson DL. Synthesis and biological evaluation of technetium-99m MAG3 as a hippuran replacement. *J Nucl Med.* 1986; 27:111–116.
2. Schlegel JU, Hamway SA. Individual renal plasma flow determination in 2 minutes. *J Urol.* 1976; 116:282–285.
3. Itoh K, Tsukamoto E. Kakizaki H, et al: Comparative study of renal scintigraphy with Tc-99m-mercaptoacetyltriglycine and I-123-orthoiodohippurate. *Nucl Med Commun.* 1993;14:644–652.
4. Tauxe WN, Dubovsky EV, Kidd T Jr, et al. New formulas for the calculation of effective renal plasma low. *Eur J Nucl Med*. 1982;7:51–54.
5. Russell CD, Taylor A, Eshima D. Estimation of technetium-99m-MAG3 plasma clearance adults from one or two blood samples. *J Nucl Med.* 1989;30:1955–1959.
6. Gjedde A. High- and low-affinity transport of D-glucose from blood to brain. *J Neurochem.* 1981;36:1463–1471.
7. Patlak CS, Blasbearg RG. Graphical evaluation of blood-to-brain transfer constants from multiple-time uptake data. *J Cereb Blood Flow Metabol.* 1985; 5:584–590.
8. Aburano T, Shuke N, Yokoyama K, et al. Renal perfusion with Tc-99m DTPA—simple noninvasive determination of extraction fraction and plasma flow. *Clin Nucl Med.* 1993;18:573–577.
9. Fujita T. Blood volume in circulation. *Respir Circ.* 1970; 18:13–24.
10. Chang LT. A method for attenuation correction in radionuclide computed tomography. *IEEE Trans Nucl Sci.* 1978; NS-25:638–643.
11. Akahira H, Konagai H, Shimoyama H, et al. Application of Rutland method by dynamic ECT with Tc-99m-DTPA, *J Nucl Med Technol.* 1993;13:133–140.